Emerging charge state after grazing collisions of heavy ions on SnTe surfaces

C. C. Montanari,[1] M. S. Gravielle,[1,2] V. D. Rodríguez,[1,2] and J. E. Miraglia[1,*]
[1]*Instituto de Astronomía y Física del Espacio, Consejo Nacional de Investigaciones Científicas y Técnicas, Casilla de Correo 67, sucursal 28, 1428 Buenos Aires, Argentina*
[2]*Departamento de Física, Facultad de Ciencias Exactas y Naturales, Universidad Nacional de Buenos Aires, Buenos Aires, Argentina*
(Received 19 July 1999; published 6 January 2000)

Emerging charge states of He and Li ions impinging with grazing incidence on a SnTe surface are calculated at high impact velocities. The charge state distribution is obtained as result of the interplay of two atomic processes: electron capture from bound states of the topmost surface atoms and electron loss from the bound states of the projectile due to collisions with the surface atoms. At high energies we find that the projectile leaves the surface with a charge state larger than the quasiequilibrium charge state reached in the vicinity of the surface. We explain this behavior in terms of the different ranges of capture and loss mechanisms. As the projectile escapes from the surface, the balance between these two processes is broken: capture is no longer effective, and loss survives ionizing the projectile. Comparisons with the experiments are presented and discussed.

PACS number(s): 34.50.Dy, 34.50.Bw

I. INTRODUCTION

The study of ion-solid collisions provides an important link between atomic physics and condensed matter physics. Comparative analysis of ion-atom, ion-solid (transmission) and ion-surface (glancing incidence) collisions gives us useful information about the structure of the solid, and it is of great interest for a systematic and comprehensive understanding of the interactions between ions and matter. In this article we present a theoretical calculation of the emerging charge fractions in grazing ion-surface collisions at high impact velocities. The incident angles under consideration are small enough for the ion not to penetrate into the solid before being reflected specularly.

The theoretical description of charge state distributions has recently received considerable attention [1–6]. At high impact velocities the emerging charge state of the ion can be considered as a consequence of the interplay of two atomic processes: electron capture from the bound states of the topmost atoms of the surface, and electron loss from the bound states of the projectile due to collisions with the surface atoms. This standard approach to deal with the problem is employed in this work.

We will concentrate on grazing collisions of He and Li ions with SnTe(100) surfaces at different incident angles for intermediate and high energies. These collisional systems have been experimentally studied [2–5]. The present theoretical description of the problem is a combination of the eikonal impulse approximation (EI) [7,8] for capture, and the multipole expansion defined in one center (MEDOC) [9,10] for electron loss, as applied to atomic collisions. The application of these theoretical models to ion-surface collisions follows the traditional way [11,12]. The work is organized as follows. In Sec. II, we develop the theoretical model and present the approximations used to describe the ion trajectory and to calculate electron capture and loss probabilities. Tables for the cross sections corresponding to He and Li ions impinging on Sn, Te, and Sb atoms are also presented. In Sec. III we display and discuss the results, and in Sec. IV the conclusions of the present article are summarized. Atomic units are used except where otherwise stated.

II. THEORY

Let us consider a heavy projectile (of charge Z_P, mass M_P and initial velocity v) impinging grazingly on a solid surface with an incident angle θ_i, as shown in Fig. 1. The charge state of the impinging ion during the collision is determined by capture and loss processes. For a given charge state j $(0 \leqslant j \leqslant Z_P)$ of the projectile, the time-dependent evolution of the charge fraction F_j is governed by the system of coupled equations

$$\frac{dF_j}{dt} = v_x \sum_k \left[F_k P_{kj}(z) - F_j P_{jk}(z) \right], \tag{1}$$

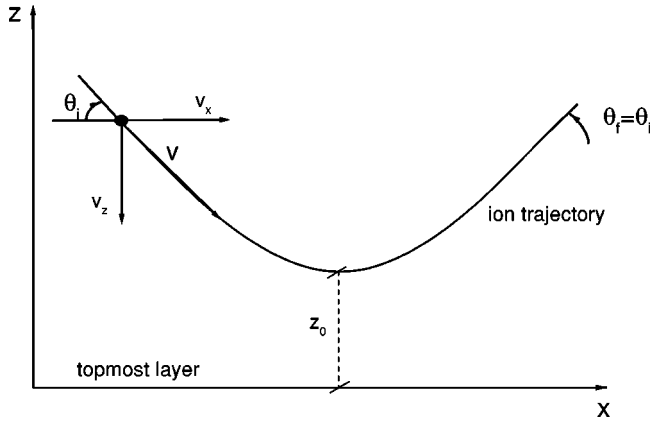

FIG. 1. Coordinate system and schematical ion trajectory for a grazing collision.

*Also at Universidad Nacional de La Matanza, La Matanza, Argentina.

where v_x is the component parallel to the surface of the impact velocity, and t is the time. The first term of the summatory represents the processes populating the charge state j, and the second term takes account of the processes depopulating j. If the ion charge changes $k \to j$, the transition probability per unit path length $P_{kj}(z)$ for a trajectory nearly parallel to the surface ($v_x \simeq v$), at a distance z of the topmost layer, is approximated [11,12] by

$$P_{kj}(z) = \delta_S \int_{-\infty}^{\infty} |A_{kj}(\rho = \sqrt{y^2+z^2})|^2 dy, \tag{2}$$

where y is the coordinate parallel to the surface and perpendicular to the velocity, $|A_{kj}(\rho)|^2$ is the impact-parameter-dependent transition probability in a single collision of the projectile with a target atom, and δ_S is the density of target atoms per unit area in the first atomic layer ($\delta_S = 1/d^2 = 0.0280$ a.u. for SnTe [1], where $d = 5.98$ a.u. is the nearest-neighbor distance).

Following Lucas [13] we have found it convenient to solve the differential Eqs. (1) in terms of the parameter $\tau = \sqrt{z^2 - z_0^2}$ instead of t, where z_0 is the distance of closest approach to the surface, and $\tau \in (-\infty, \infty)$. Then the charge state equations are

$$\frac{dF_j}{d\tau} = a(\tau) \sum_k [F_k P_{kj}(\tau) - F_j P_{jk}(\tau)], \tag{3}$$

where the coefficient $a(\tau)$ is

$$a(\tau) = \sqrt{\frac{\tau^2}{z_0^2 + \tau^2}} \, \frac{v_x}{|v_z(\tau)|}, \tag{4}$$

and v_z is the component normal to the surface of the projectile velocity.

It is convenient to introduce the range $\langle z \rangle_{kj}$ of the transition probability P_{kj}. We estimate this range as twice the mean z value,

$$\langle z \rangle_{kj} = 2 \frac{\int_0^{\infty} z \, P_{kj}(z) \, dz}{\int_0^{\infty} P_{kj}(z) \, dz}. \tag{5}$$

As we shall see, the emerging charge state can be explained in terms of the comparative values of electron capture and loss ranges. Next we summarize the approximations made in this work.

A. The trajectory

Figure 1 displays the ion path for a specular reflection ($\theta_f = \theta_i$) from the SnTe(100) surface. The surface lays on the (x,y) plane and the projectile moves in the direction of the positive x axis. The jellium edge in the SnTe is displaced from the topmost atomic layer by $z = 2.99$ a.u. [1]. As usual, it is assumed that the projectile undergoes an elastic collision with the surface, and $v_x \simeq v$ does not change during the collision. The velocity component normal to the surface is obtained assuming conservation of energy in the transversal direction, E_t, in the form

$$E_t(\theta_i) = \frac{1}{2} M_P (v \sin\theta_i)^2 = \frac{1}{2} M_P v_z^2 + V_{SP}(z), \tag{6}$$

where $V_{SP}(z)$ is the interaction potential between the projectile and the surface. To describe this interaction we consider an averaged Moliere potential [12], given by

$$V(z) = 2\pi \delta_S \overline{Z}_T Z_P \sum_{i=1}^{3} \frac{\alpha_i}{\beta_i} e^{-\beta_i z}, \tag{7}$$

with the Moliere parameters [14] $\alpha_i = (0.35,\ 0.55,\ 0.1)$, $\beta_i a_{TF} = (0.3,\ 1.2,\ 6.0)$ and the Thomas-Fermi screening parameter $a_{TF} = 0.885/(Z_P^{1/2} + \overline{Z}_T^{1/2})^{2/3}$. In agreement with Juaristi *et al.* [12] we find that the ion trajectory is almost the same if we use the Ziegler-Biersack-Littmark (ZBL) potential [15] instead of the Moliere one. Thus, our charge fraction results change very little (less than 1%) using any of these potentials as V_{SP}. The target charge $\overline{Z}_T$ corresponding to the SnTe surface is approximated by $\overline{Z}_T = (Z_{Sn} + Z_{Te})/2 = 51 = Z_{Sb}$, which is a good approximation since the nuclear charges of Sn and Te are very similar ($Z_{Sn} = 50$ and $Z_{Te} = 52$). The image potential is not taken into account because it is negligible in the high velocity regime considered here [12].

The turning point of the trajectory z_0 is obtained from Eq. (6) considering $E_t(\theta_i) = V_{SP}(z_0)$. We analyzed collisions at glancing angles smaller than a critical one θ_c, which results from equating $E_t(\theta_c) = V_{SP}(z_0 = 0)$.

B. Capture cross probabilities

We consider capture processes by single collisions of He and Li ions with neutral Sn and Te atoms. The approximation used to describe these processes is the prior version of the eikonal impulse approximation [7]. This is a distorted wave method that uses the eikonal wave function in the initial channel and the exact impulse wave function in the final channel. This method has already proved to be successful in dealing with a wide variety of atomic collisions in the intermediate and high energy range [8].

Partial capture cross sections from n=4 shell of Sn and Te atoms into the ground state of the projectile are shown in Table I and Table II for He and Li ions, respectively. We consider capture from the valence electrons as coming from the $n = 5$ atomic bound state. In the case of He ions, capture cross sections from this shell contribute to the total cross section (averaging Sn and Te) about ten percent at the velocities considered here, with the contribution being higher for Te targets than for Sn ones. In the case of Li ions, we obtain capture cross sections from $n = 5$ shell much smaller than those from $n = 4$, and are thus neglected. Total cross sections shown in Tables I and II are obtained by adding the partial cross sections to the ground state and using the Openheimer rule [16] to take into account capture into excited states. For He and Li projectiles, the most important contri-

TABLE I. Capture and loss cross sections $\sigma_{i\ i\pm1}$ for the projectile charge changing $i \rightarrow i \pm 1$ in the collision of He^{+i} ions impinging on Sn, Te and Sb atoms. Atomic units are used. Numbers in brackets represent powers of 10.

	v (a.u.)	3.16	3.87	4.47
Sn	$\sigma_{10}(4s)$	3.98[-4]	3.47[-4]	5.28[-4]
	$\sigma_{10}(4p)$	1.11[-2]	8.57[-3]	6.13[-3]
	$\sigma_{10}(4d)$	3.97[-1]	2.64[-1]	1.56[-1]
	$\sigma_{10}(5s)$	9.43[-3]	4.30[-3]	2.71[-3]
	$\sigma_{10}(5p)$	2.65[-2]	7.65[-3]	2.44[-3]
	σ_{10}(total)	5.34[-1]	3.42[-1]	2.02[-1]
Te	$\sigma_{10}(4s)$	4.59[-4]	3.21[-4]	3.84[-4]
	$\sigma_{10}(4p)$	5.83[-3]	5.34[-3]	4.37[-3]
	$\sigma_{10}(4d)$	1.78[-1]	1.31[-1]	9.30[-2]
	$\sigma_{10}(5s)$	9.99[-3]	4.61[-3]	3.20[-3]
	$\sigma_{10}(5p)$	7.53[-2]	2.73[-2]	1.04[-2]
	σ_{10}(total)	3.24[-1]	2.03[-1]	1.34[-1]
Sn	$\sigma_{21}(4s)$	7.60[-4]	5.30[-4]	7.44[-4]
	$\sigma_{21}(4p)$	2.66[-2]	1.61[-2]	1.18[-2]
	$\sigma_{21}(4d)$	7.08[-1]	4.26[-1]	2.41[-1]
	$\sigma_{21}(5s)$	2.99[-2]	1.28(-2]	6.87[-3]
	$\sigma_{21}(5p)$	2.98[-2]	8.61[-3]	2.78[-3]
	σ_{21}(total)	9.56[-1]	5.58[-1]	3.16[-1]
Te	$\sigma_{21}(4s)$	7.88[-4]	5.80[-4]	4.62[-4]
	$\sigma_{21}(4p)$	1.45[-2]	9.85[-3]	7.47[-3]
	$\sigma_{21}(4d)$	2.65[-1]	1.95[-1]	1.43[-1]
	$\sigma_{21}(5s)$	3.37[-2]	1.51[-2]	8.75[-3]
	$\sigma_{21}(5p)$	1.07[-1]	3.56[-2]	1.26[-2]
	σ_{21}(total)	5.06[-1]	3.08[-1]	2.07[-1]
Sb	σ_{01}(total)	1.77[+1]	1.62[+1]	1.49[+1]
	σ_{12}(total)	5.76[0]	5.46[0]	5.32[0]

TABLE II. Capture and loss cross sections $\sigma_{ii\pm1}$ for the projectile charge changing $i \rightarrow i \pm 1$ in the collision of Li^{+i} ions impinging on Sn, Te and Sb atoms. Atomic units are used. Numbers in brackets represent powers of 10.

	v (a.u.)	4.47	6.00
Sn	$\sigma_{21}(4s)$	2.80[-3]	1.58[-3]
	$\sigma_{21}(4p)$	3.70[-2]	1.39[-2]
	$\sigma_{21}(4d)$	3.38[-1]	7.60[-2]
	σ_{21}(total)	4.54[-1]	1.10[-1]
Te	$\sigma_{21}(4s)$	1.56[-3]	1.14[-3]
	$\sigma_{21}(4p)$	2.47[-2]	1.10[-2]
	$\sigma_{21}(4d)$	1.75[-1]	6.77[-2]
	σ_{21}(total)	2.42[-1]	9.59[-2]
Sn	$\sigma_{32}(4s)$	5.83[-3]	2.24[-3]
	$\sigma_{32}(4p)$	6.45[-2]	2.39[-2]
	$\sigma_{32}(4d)$	3.84[-1]	7.36[-2]
	σ_{32}(total)	5.46[-1]	1.20[-1]
Te	$\sigma_{32}(4s)$	3.70[-3]	1.81[-3]
	$\sigma_{32}(4p)$	4.51[-2]	1.80[-2]
	$\sigma_{32}(4d)$	2.36[-1]	7.16[-2]
	σ_{32}(total)	3.42[-1]	1.10[-1]
Sb	σ_{12}(total)	8.96[0]	6.51[0]
	σ_{23}(total)	3.37[0]	3.12[0]

bution to the total cross section comes from capture processes from the 4*d* subshell. Noticeably, as observed from the Tables, the results for capture from Sn and Te atoms are different in spite of their similar nuclear charge. Capture probabilities ranges $\langle z \rangle_{Z_P, Z_P-1}$ are displayed in Table III.

C. Electron loss probabilities

Electron loss probabilities are calculated by solving numerically the time dependent Schrödinger equation in the impact parameter formalism, using the MEDOC approximation [9]. In this method the wave function is developed as a combination of a target centered multipolar expansion for the angular part, and a discretization of the radial part into a finite size box. By using a complex coordinate technique, we have avoided problems arising from reflections at the boundary [10]. The virtue of this method, as applied here, is that in the present problem the charge exchange channel is closed, and a single centered multipolar expansion is appropriate for all the impact energies under consideration. The maximum angular momentum in the expansion is $L_{max}=6$. The electron loss probability in the impact parameter formalism, $P_{el}(\rho)$, is obtained by two alternative ways. First, they are calculated by projecting the collisional wave function over continuum states and then by adding all these contributions. Second, the total excitation probability $P_{exc}(\rho)$ is calculated and, afterwards, the electron loss probability is obtained by simply using $P_{el}(\rho)=1-P_{exc}(\rho)$. Both methods agree within 30% with the latter method being the most reliable for small impact parameters (where $P_{exc} \ll 1$), and the former method for large impact parameters (where $P_{el} \ll 1$).

The formalism presented above considers only one electron. In the case of ions with two electrons, we use the same description by employing an ion effective charge, which is calculated to give the correct Hartree-Fock energy for the initial 1*s* state [17].

The potential $V(r)$ used to describe the interaction between a surface atom and an electron bound to the projectile is a critical point. Three different potentials were studied, as posed next. Any of these three potentials produce results rather insensitive to the target nuclear charge, so we have simply considered the target as composed by Sb atoms, leaving 5 electrons per atom to the valence band. The potentials studied are:

(i) the ZBL potential [15] giving by

$$V_{ZBL}(r) = -\frac{Z_T}{r} \sum_{i=1}^{4} \alpha_i e^{-\beta_i r}, \tag{8}$$

TABLE III. Emerging charge fractions F_j for incident He^+ and Li^+ projectiles on SnTe surfaces. The incident angle considered is the angle of maximum approach to the surface θ_c. Values of the equilibrium charge fractions in collisions through the SnTe solid are presented for comparison. Also displayed, the range of capture and loss probabilities $\langle z\rangle_{kj}$ for the projectile charge changing $k\rightarrow j$.

He^+			
v (a.u.)	3.16	3.87	4.47
θ_c (mrad)	13.0	10.6	9.21
F_1 (surf.)	0.11	0.055	0.029
F_2 (surf.)	0.89	0.94	0.97
F_1 (sol.)	0.11	0.073	0.047
F_2 (sol.)	0.88	0.92	0.95
$\langle z\rangle_{12}$	1.74	1.61	1.52
$\langle z\rangle_{21}$	1.60	1.46	1.28
Li^+			
v (a.u.)	4.47	6.0	
θ_c (mrad)	8.46	6.30	
F_2 (surf.)	0.12	0.031	
F_3 (surf.)	0.87	0.97	
F_2 (sol.)	0.12	0.035	
F_3 (sol.)	0.88	0.96	
$\langle z\rangle_{23}$	1.26	1.09	
$\langle z\rangle_{32}$	1.34	1.04	

where the parameters are $\alpha_i=(0.0282, 0.280, 0.510, 0.182)$, $\beta_i\, a_{ZBL}=(0.202, 0.403, 0.942, 3.20)$ and $a_{ZBL}=0.885/(Z_P^{0.23}+Z_T^{0.23})$.

(ii) The Moliere potential [14], which has the same structure as Eq. (8) but only three terms, with the coefficients α_i and β_i as given below Eq. (7). Both ZBL and Moliere potentials include the interaction of the projectile electron with the valence band electrons as belonging to the target atom.

(iii) As a third case, we consider the two parameter Garvey potential [1,18] V_G to describe the interaction with the core ionic atom of Sb^{5+}, and the free electron gas potential V_{feg} to take into account the interaction with the outer 5 electrons. The potential V_{feg} is created by a sphere of constant charge density $\delta_e=-5/d^3=-0.0234$ a.u. and a radius equal to the Wigner-Seitz radius $r_e=[3d^3/4\pi]^{1/3}=3.71$ a.u. The total interaction potential is then $V_{G+feg}=V_G+V_{feg}$, given by

$$V_G(r)=\frac{(Z_T-5)}{r}[1-\Omega(r)]-\frac{Z_T}{r} \tag{9}$$

and

$$V_{feg}=\begin{cases}\dfrac{2}{3}\pi\delta_e r^2-2\pi r_e^2\delta_e & \text{if } r\leqslant r_e\\ 5/r & \text{if } r\geqslant r_e\end{cases}. \tag{10}$$

with $Z_T=51$ and $[\Omega(r)]^{-1}=2.710[\exp(2.039\,r)-1]+1$ [18].

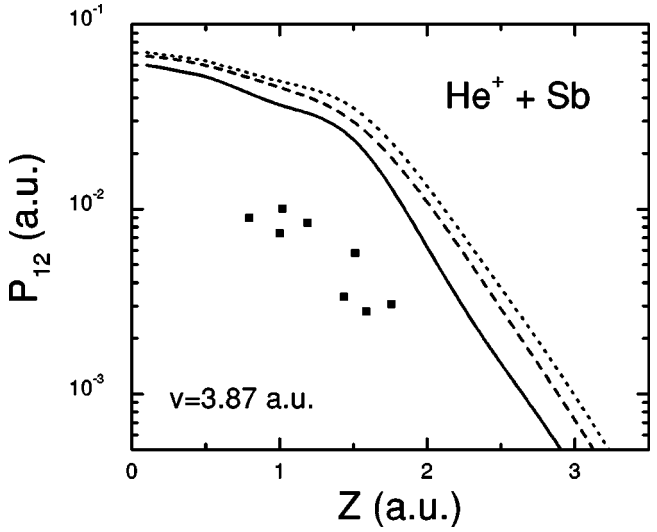

FIG. 2. Electron loss probability per unit path length for 1.5 MeV $He^+ + Sb$ collision, as a function of the distance to the surface topmost layer z. Results obtained using different atom-electron potentials are displayed. Symbols: solid line, ZBL potential; dashed line, Moliere potential; dotted line, Garvey potential for the interaction with the ionic core and the valence electrons represented by a constant density sphere. Squares, experimentally derived values of Fujii *et al.* [2].

We use these three potentials to obtain electron loss probabilities per unit path length. Results of P_{12} for 1.5 MeV He^+ ions impinging on a Sb surface are plotted in Fig. 2. Though no substantial changes are obtained in the total cross sections, differences in the probabilities at intermediate impact parameters (between 1 and 2 a.u.) lead to important differences at the level of the emerging charge fractions (up to 40% for the emerging charge fraction of He^+, F_1). Hereafter we will restrain our calculations to the ZBL potential which shows a better performance in comparing with the experiments in Fig. 2.

For 0.3-MeV/amu Li ions, our electron loss probabilities are in good agreement with the Classical Trajectory Monte Carlo (CTMC) values as reported by Reinhold *et al.* [1].

We have not taken into account antiscreening processes [19] in our calculations. By considering these processes the electron loss probabilities would increase and the loss cross sections would be bigger than those given in Tables I and II. The antiscreening contribution is known to be relevant at large impact parameters but negligible at short distances [20]. Instead, our charge state results depend strongly on the values of $P_{kj}(z)$ at $z<2$ a.u., and they change very little for $z>2$ a.u. Thus, antiscreening will leave a trace in the outgoing charge state only if it is appreciable at distances as small as 2 a.u. In Ref. [1], the antiscreening is taken into account by including the interaction of the projectile electron with the quasifree target electrons. As can be seen in Fig. 9 of Ref [1], its contribution is appreciable for $z\geqslant 2$ a.u. and the outgoing emerging charge fractions are rather independent of this consideration (they change less than 4%).

Loss cross sections values are shown in Table I and Table II for He and Li ions, respectively. The corresponding probabilities ranges $\langle z\rangle_{Z_p-1,Z_p}$ are displayed in Table III.

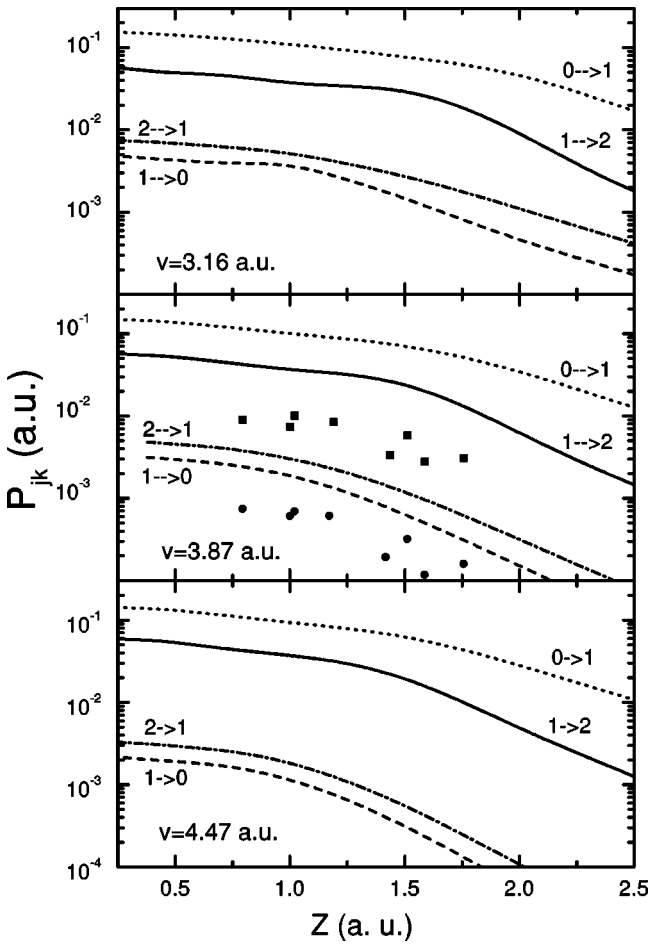

FIG. 3. Transition probabilities per unit path length for He^{+j} + SnTe collision, as a function of the distance to the surface topmost layer z, when the projectile charge changes $j \rightarrow k$. Impact velocities are shown in the figure. Symbols: squares (P_{12}) and circles (P_{21}), experimentally derived values of Fujii *et al.* [2].

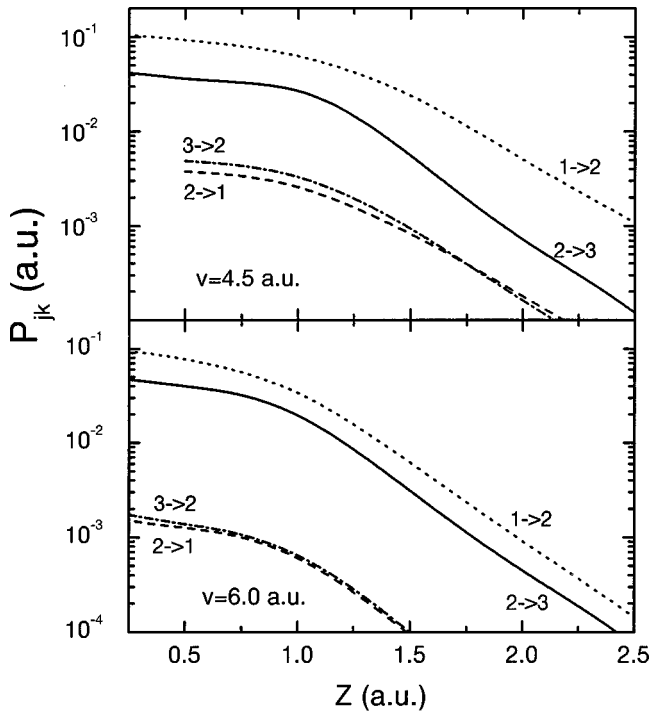

FIG. 4. Similar to Fig. 3 for Li^{+j} + SnTe collision.

III. RESULTS AND DISCUSSION

Transition probabilities per unit path length $P_{kj}(z)$ calculated from Eq. (2) are shown in Figs. 3 and 4 for He and Li ions respectively, impinging on the SnTe surface. They are plotted as a function of the distance z to the surface topmost layer. In Fig. 3 we note that, for He ions, electron loss probabilities do not change appreciably with the ion impact velocity while the electron capture probabilities fall as the velocity increases. This can also be observed in Table III where the ranges are $\langle z \rangle_{12} > \langle z \rangle_{21}$, and the decreasing tendency with the velocity is greater for capture than for loss ranges. This is a fundamental point to understand the difference between the emerging charge state from the surface and the quasi-equilibrium charge state very close to the surface. In Fig. 3 we also display the electron capture (P_{21}) and electron loss (P_{12}) probabilities as reported by Fujii *et al.* [2] for 1.5 MeV impact energy. These experimentally derived values fall bellow our theoretical curves. Noticeably the difference between our calculations and Fujii *et al.* [2] results, about a factor five, is the same for loss and capture probabilities, and it leaves almost no trace at the level of the charge state fractions. Nevertheless, this large discrepancy needs some comments. The values shown in Figs. 2 and 3 are not experimental measures but derived values from the observed charge state fractions and energy losses at different emerging angles. Fujii *et al.* [2] obtained the position-dependent probabilities by using a master equation formulation and the hypothesis of deflection in the outgoing angles due to steps in the surface. We cannot explain the origin of the discrepancy between these experimentally derived values and our calculations; it can be a hint that the interaction model is missing some important physical contribution, or a problem of normalization of the experimental results.

In Fig. 4 we can observe that, for Li ions, capture and loss probabilities have similar ranges (they differ from each other less than 6%) at the velocities considered. However, the decreasing tendency of capture range with the velocity is greater than that of loss range. Note from Table III the differences in $\langle z \rangle$ between He and Li ions, which will be useful to understand the corresponding differences in the charge fractions behavior along the trajectory.

In Table III we also show the values obtained for the emerging charge fractions F_j for incident He^+ and Li^{2+} projectiles on SnTe surfaces. As experimentally observed [3,4,6], the emerging charge fractions are independent of the incident charge state of the ion. This behavior indicates that the memory of the entrance charge state is lost by the time the projectile reaches the surface. The incident angle considered is the angle of maximum approach to the surface θ_c, for which $z_0 = 0$. For incident He^+ (Li^{2+}) ions, the F_0 (F_1) values obtained are less than 0.1% (0.3%), so they are not displayed.

In Figs. 5 and 6 we plot the ratio of charge fractions F_{Z_p-1}/F_{Z_p} as a function of the distance to the surface top-

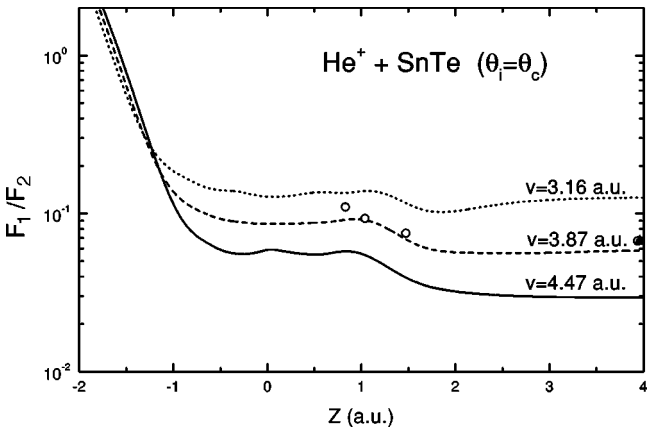

FIG. 5. Ratio of charge fractions F_{Z_P-1}/F_{Z_P} for He^+ projectiles impinging grazingly on the SnTe surface, as a function of the distance z to the surface topmost layer. The incident angle is θ_c. For clarity the entrance channel is denoted with negative values of z. The different impinging velocities are displayed in the figure. They are compared with Fujii *et al.* results. Symbols: open circles, experimentally derived values [4]; closed triangle, experimental value [2], at $v=3.87$ and $\theta_i=5.7$ mrad.

most layer z, for He and Li ions, respectively. We denote the entrance channel with negative values of z. The incident angle considered is θ_c, but the results are rather insensitive to the incident angle for $\theta_i \geqslant 0.4\theta_c$, as can be observed in Figs. 7 and 8.

For He ions, Fig. 5 shows that at intermediate impact velocities the ion gets an equilibrium charge state close to the surface, which remains almost constant until exit. Instead, at high impact velocities, the charge state gets a quasi-equilibrium value in the immediate vicinities of the surface, but it tends to another value far from the surface. The discrepancy between these two values is due to the different ranges of electron capture and loss probabilities at high velocities (see Table III). Close to the surface topmost layer both mechanisms are present, but at a certain distance capture loses its effectiveness while electron loss still ionizes the

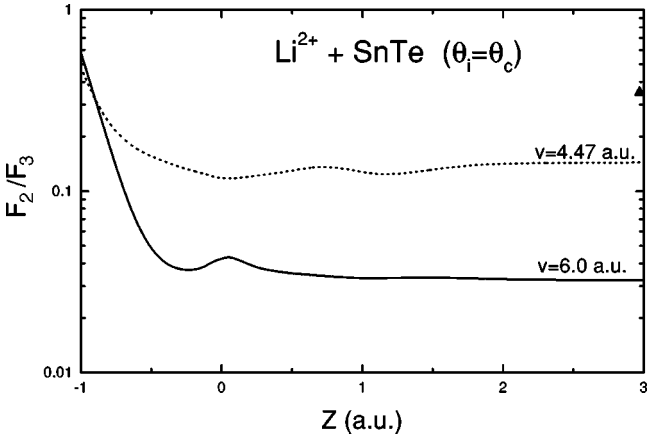

FIG. 6. Similar to Fig. 5 for Li^{2+} projectiles impinging grazingly on the SnTe surface. Symbols: closed triangle, experimental result of Kimura *et al.* [3] for impact velocity $v=4.47$ and $\theta_i=6.0$ mrad.

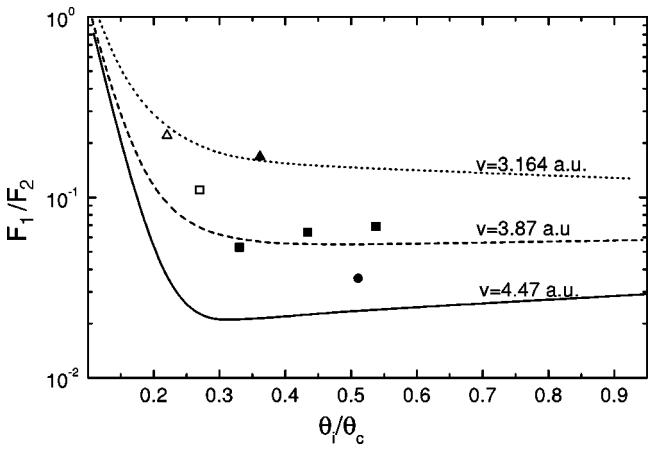

FIG. 7. Ratio of charge fractions F_{Z_P-1}/F_{Z_P} for the $He^+ + SnTe$ collision, as a function of the incident angle θ_i normalized to the angle of maximum approach to the surface θ_c. Symbols: closed triangles, squares, and circles, experimental results of Fujii *et al.* [2] at $v=3.16$, 3.87, and 4.47, respectively. Open triangle and square, experimental results of Kimura *et al.* [5] at $v=3.16$ and 3.87, respectively.

projectile. Thus, the emerging charge state of the projectile is bigger than that obtained in the surface vicinity, and this behavior becomes more pronounced as the velocity increases. In Fig. 5 we have also displayed the experimental value of F_1/F_2 far from the surface, and the experimentally derived results near the surface as reported by Fujii *et al.* in Refs. [2] and [4], respectively. The velocity for these experiments is $v=3.87$ and the incident angle $\theta_i=5.7$ mrad. Though this is not the angle θ_c considered in this figure, this value is in the region $\theta_i \geqslant 0.4\theta_c$ where the charge fractions change very little with the angle.

In Fig. 6 we observe that, for Li ions, the charge fraction reaches a value close to the surface, which almost remains until exit. This behavior is in accordance with the similar ranges of electron capture and loss probabilities of Table III. In Fig. 6 we include Kimura *et al.* [3] experimental results for $v=4.47$ and incident angle $\theta_i=6.0$ mrad. Again the experimental incident angle is in the region $\theta_i \geqslant 0.4\theta_c$.

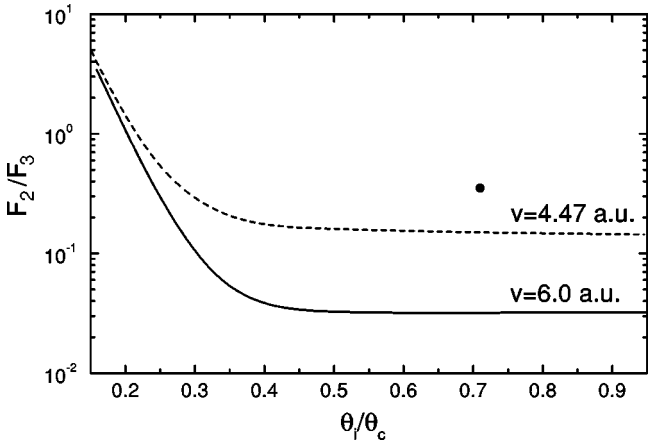

FIG. 8. Similar to Fig. 7 for $Li^{2+} + SnTe$ collision. Closed circle, experimental value of Kimura *et al.* [3] at $v=4.47$.

In Fig. 7 we plot the ratio of emerging charge fractions F_1/F_2 for He impact on the SnTe surface, as a function of the ion incident angle. This curve shows reasonable agreement with the experimental values of Fujii *et al.* [2,4] and Kimura *et al.* [5], for $v=3.16$ and $v=3.87$, and are below the experimental value for $v=4.47$. As already mentioned, these results are almost insensitive to the ion incident angle for $\theta_i \geqslant 0.4\theta_c$, in agreement with Fujii *et al.* [4] observations. For Li ions, the same tendency is observed in Fig. 8. In this case, the theoretical results are compared with Kimura *et al.* [3] measures of F_2/F_3 at v=4.47, being the experimental value a factor two higher than our result . At higher velocities there are no data available.

Two points should be remarked about these figures:

(i) First, as the projectile gets very close to the surface, the fraction remains around a constant which happens to be

$$\frac{F_{Z_P}}{F_{Z_P-1}} \simeq \frac{P_{Z_P-1,Z_P}(z=0)}{P_{Z_P,Z_P-1}(z=0)}. \tag{11}$$

This expression can be deduced from Eq. (1) using that the trajectory is parallel to the surface at the closest approach, and the probabilities per unit path length are almost constant and near to the value at the origin. The differential equations for the charge fractions through the solid are the same as Eq. (1) changing probabilities per unit path length (P_{kj}) by cross sections (σ_{kj}). Note the difference between Eqs. (11) and the equilibrium charge fractions within solids given by

$$\frac{F_{Z_P}}{F_{Z_P-1}} \simeq \frac{\sigma_{Z_P-1,Z_P}}{\sigma_{Z_P,Z_P-1}}. \tag{12}$$

In Table III we observe that, at the lowest velocity considered in this work, the ratio of emerging charge fractions far from the surface is similar to the equilibrium charge fraction within solids, i.e., $(F_{Z_P}/F_{Z_P-1})_{surface} \approx (F_{Z_P}/F_{Z_P-1})_{solid}$. This is a numerical coincidence that is not longer valid for increasing velocities, where we obtain $(F_{Z_P}/F_{Z_P-1})_{surface} > (F_{Z_P}/F_{Z_P-1})_{solid}$.

(ii) Second and more important, at high velocities, when the projectile escapes from the surface the balance between capture and loss processes is broken. Capture is no longer effective while loss survives ionizing the projectile. Thus, the projectile comes out of the surface with a charge state larger than that reached at the origin. This behavior is a consequence of the difference between capture and loss ranges, being more evident at larger velocities. For He ions, this difference in the ranges is observed at the higher velocities considered here, together with the mentioned consequences at the level of the charge fractions. Instead, for Li ions, we have not reached the high velocity region where the capture range is smaller than the loss one. This is consistent with the fact that Li emerging charge fractions are similar to the charge fractions close to the surface. However, for impact velocities higher than those considered here, the decreasing tendency of capture ranges with the velocity makes it reasonable to expect a similar behavior to that observed for He ions.

IV. CONCLUSIONS

We have calculated charge fractions in grazing collisions of He and Li ions with a SnTe(100) surface. For He ions we have obtained acceptable agreement with the experimental results of Kimura and collaborators [2,4,5]. At intermediate impact velocities we find that the ion gets an equilibrium charge state close to the surface, which remains nearly the same until exit. Instead, at high impact velocities, the charge state tends to another value far from the surface. The discrepancy between these two values is due to the different ranges of electron capture and loss processes. Close to the surface topmost layer both mechanisms are present, but at a certain distance capture turns off and only electron loss survives. Thus, the emerging charge state of the projectile is bigger than that obtained in the surface vicinity, and this behavior becomes more remarkable when the velocity increases. This conclusion is in agreement with experimentally derived calculations of Fujii *et al.* [4]. The same tendency for the charge state in the surface vicinity has also been reported by Fritz *et al.* [6] who measured charge fractions in grazing collisions of C^{4+} with the SnTe surface.

Instead, for Li ions at the velocities considered in this work, we find that charge fractions get a value close to the surface, which remains until exit. Again this behavior is due to the ranges of electron capture and loss probabilities that, in this case, are of the same order. However, for impact velocities higher than those considered here, we expect a behavior similar to that observed for He ions. Experimental results at such velocities are not available in the literature up to now.

ACKNOWLEDGMENTS

We are indebted to Dr. K. Kimura and Dr. R. Minitti for useful discussions.

[1] C. O. Reinhold and J. Burgdörfer, Phys. Rev. A **55**, 450 (1997).
[2] Y. Fujii, S. Fujiwara, K. Narumi, K. Kimura, and M. Mannami, Phys. Rev. A **49**, 1897 (1994).
[3] K. Kimura, T. Kishi, and M. Mannami, Nucl. Instrum. Methods Phys. Res. B **90**, 282 (1994).
[4] Y. Fujii, S. Fujiwara, K. Kimura, and M. Mannami, Nucl. Instrum. Methods Phys. Res. B **58**, 18 (1991).
[5] K. Kimura, Y. Fujii, M. Hasegawa, Y. Susuki, and M. Mannami, Phys. Rev. B **38**, 1052 (1988).
[6] M. Fritz, K. Kimura, Y. Kuroda, and M. Mannami, Phys. Rev. A **54**, 3139 (1996).
[7] M. S. Gravielle and J. E. Miraglia, Phys. Rev. A **44**, 7299 (1991).
[8] M. S. Gravielle and J. E. Miraglia, Phys. Rev. A **51**, 2131 (1995); **52**, 851 (1995).
[9] A. Salin, Phys. Rev. A **36**, 5471 (1987).
[10] V. Rodriguez and A. Salin, J. Phys. B **25**, L467 (1992).

[11] M. S. Gravielle and J. E. Miraglia, Phys. Rev. A **50**, 2425 (1994).
[12] J. I. Juaristi, F. J. García de Abajo, and P. M. Echenique, Phys. Rev. B **53**, 13 839 (1996).
[13] A. A. Lucas, Phys. Rev. B **20**, 4990 (1979).
[14] I. M. Torrens, *Interatomic Potentials*, Academic Press, New York (1972).
[15] J. F. Ziegler, J. P. Biersack, and U. Littmark, *The Stopping and Range of Ions in Matter*, edited by J. F. Ziegler (Pergamon, New York, 1985), Vol. 1.
[16] M. R. C. McDowell and J. P. Coleman, *Introduction to the Theory of Ion-Atom Collisions* (North-Holland, Amsterdam 1970).
[17] E. Clementi and C. Roetti, At. Data Nucl. Data Tables **14**, 177 (1974).
[18] R. H. Garvey, C. H. Jackman, and A. E. S. Green, Phys. Rev. A **12**, 1144 (1975).
[19] E. C. Montenegro and W. E. Meyerhof, Phys. Rev. A **43**, 2289 (1991).
[20] A. B. Voitkiv, G. M. Sigaud, and E. C. Montenegro, Phys. Rev. A **59**, 2794 (1999).